

Triribbed-Functionalized Clathrochelate Iron(II) Dioximates as a New and Promising Tool To Obtain Polynucleating and Polynuclear Compounds with Improved Properties

Yan Z. Voloshin,^{*,†} Oleg A. Varzatskii,[‡] Tatyana E. Kron,[†] Vitaly K. Belsky,[†]
Valery E. Zavodnik,[†] Nataly G. Strizhakova,[‡] and Alexey V. Palchik[‡]

Karpov Institute of Physical Chemistry, 103064 Moscow, Russia, and Institute of General and Inorganic Chemistry, 252142 Kiev, Ukraine

Received May 4, 1999

Template condensation on iron(II) ion of dichloroglyoxime (H₂Cl₂Gm) with (C₆H₅O)₃, *n*-C₄H₉B(O-*n*-C₄H₉)₂, and BF₃·O(C₂H₅)₂ in CH₃NO₂ afforded reactive clathrochelate precursors Fe(Cl₂Gm)₃(BC₆H₅)₂ (**2**), Fe(Cl₂Gm)₃(B-*n*-C₄H₉)₂ (**3**), and Fe(Cl₂Gm)₃(BF)₂ (**4**). A series of triribbed-functionalized clathrochelate dioximates have been synthesized. Reaction of **2** with C₆H₅SH/K₂CO₃ and CH₃SH/*t*-C₄H₉OK in 1,4-dioxane and THF afforded Fe((C₆H₅S)Gm)₃(BC₆H₅)₂ (**5**) and Fe((CH₃S)Gm)₃(BC₆H₅)₂ (**6**). Reaction of **3** with C₆H₅OK in THF afforded Fe((C₆H₅O)Gm)₃(B-*n*-C₄H₉)₂ (**7**). Condensation of **3** with bis(2-(*o*-oxyphenoxy))diethyl ether in THF afforded di- and tricrown etheric Fe(CwGm)₂(Cl₂Gm)(B-*n*-C₄H₉)₂ (**8**) and Fe(CwGm)₃(B-*n*-C₄H₉)₂ (**9**) clathrochelates. Condensation of **3** with 3,5-dithiaoctane-1,8-dithiol/Cs₂CO₃ in DMF afforded the thiocrown etheric Fe((12anS₄-Gm)₃(BC₆H₅)₂) complex (**10**). Reaction of **2** with *n*-butylamine in DMF resulted in the tetrasubstituted Fe(*n*-C₄H₉NH)Gm)₂(Cl₂Gm)(BC₆H₅)₂ clathrochelate (**11**). The clathrochelates obtained have been characterized both on the basis of elemental analysis, FAB and PD mass spectrometry, IR, UV–vis, ⁵⁷Fe Mössbauer, and NMR spectroscopies and crystallographically (compounds **3**, **4**, **6**, **7**, and **11**). An encapsulated iron(II) ion in a distorted trigonal-prismatic environment of six nitrogen atoms of the macrobicyclic ligand was found to be in a low-spin state. The cyclic voltammograms for the complexes **2**–**11** show irreversible oxidation waves assignable to Fe³⁺/Fe²⁺ couples. The correlation of *E*_{1/2} for these couples with Hammett σ_{para} constants for substituents in dioximate fragments has been demonstrated.

Introduction

Polynucleating ligand systems and polynuclear complexes of *d*-metals derived from them are actively being investigated as models of metalloproteins and metalloenzymes and other important biological systems (biomimetics),^{1–3} efficient catalysts for chemical reactions,⁴ and promising materials for molecular electronics (molecular magnets, switches, transistors, and wires).^{5–8} The complexes of clathrochelate ligands, representatives of recently actively studied compounds involving an encapsulated metal ion,^{9–15} have also been proposed as biomimetics,¹⁶

catalysts for photochemical and redox processes,^{17–22} electron carriers,^{23–28} high-sensitivity analytical^{29,30} and chiral reagents,^{31–33}

* To whom correspondence should be addressed.

[†] Karpov Institute of Physical Chemistry.

[‡] Institute of General and Inorganic Chemistry.

- (1) *Metalloproteins*; VCH: Weinheim, 1985.
- (2) Feig, A. L.; Lippard, S. J. *Chem. Rev.* **1994**, *94*, 759.
- (3) Holm, R. H.; Solomon, E. I., Guest Eds. *Chem. Rev.* **1996**, *96*, No. 7.
- (4) *Catalysis by Di- and Polynuclear Metal Complexes*; Cotton, F. A., Adams, R., Eds.; VCH: New York, 1997.
- (5) Kanh, O. *Molecular Magnetism*; VCH: Weinheim, 1993.
- (6) Kanh, O. *Adv. Inorg. Chem.* **1995**, *73*, 49.
- (7) Balzani, V.; Juris, A.; Venturi, M.; Campagna, S.; Serroni, S. *Chem. Rev.* **1996**, *96*, 759.
- (8) Lehn, J.-M. *Supramolecular Chemistry*; VCH: Weinheim, 1995.
- (9) Kostromina, N. A.; Voloshin, Y. Z.; Nazarenko, A. Y. *Clathrochelates: synthesis, structure, properties*; Naukova Dumka: Kiev, 1992.
- (10) Sargeson, A. M. *Chem. Br.* **1979**, *15*, 23.
- (11) Sargeson, A. M. *Pure Appl. Chem.* **1984**, *56*, 1603.
- (12) Sargeson, A. M. *Pure Appl. Chem.* **1986**, *58*, 1511.
- (13) Voloshin, Y. Z. *Russ. J. Chem.* **1998**, *42*, 5.
- (14) Burdinski, D.; Birkelbach, F.; Weyhermüller, T.; Flörke, U.; Haupt, H.-J.; Lengen, M.; Trautwein, A. X.; Bill, E.; Wieghard, K.; Chaudhuri, P. *Inorg. Chem.* **1998**, *37*, 1009.

- (15) Birkelbach, F.; Flörke, U.; Haupt, H.-J.; Butzlaff, C.; Trautwein, A. X.; Wieghard, K.; Chaudhuri, P. *Inorg. Chem.* **1998**, *37*, 2000 and references therein.
- (16) Sargeson, A. M. *Coord. Chem. Rev.* **1996**, *151*, 89.
- (17) Pat. 525243 Australia, IC3 C 07 D 487/08, C 07 B 15/022, C 07 F 9/022. *Metal complexes and their use for hydrogen peroxide production*/Hertl, A. J.; Sargeson, A. M.; Harrowfield, J. M. Publ. 28.10.82.
- (18) Mok, C.-Y.; Zanella, A. W.; Creutz, C.; Sutin, N. *Inorg. Chem.* **1984**, *23*, 2891.
- (19) Pina, F.; Mulazzani, Q. G.; Venturi, M.; Ciano, M.; Balzani, V. *Inorg. Chem.* **1985**, *24*, 848.
- (20) Königstein, C.; Mau, A. W.-H.; Osvath, P.; Sargeson, A. M. *Chem. Commun.* **1997**, 423.
- (21) Figueredo, P.; Pina, F. J. *Photochem. Photobiol. A* **1988**, *44*, 57.
- (22) Anderson, K. A.; Wherland, S. *Inorg. Chem.* **1991**, *30*, 624.
- (23) Greaser, I. I.; Sargeson, A. M.; Zanella, A. W. *Inorg. Chem.* **1983**, *22*, 4022.
- (24) Borchardt, D.; Pool, K.; Wherland, S. *Inorg. Chem.* **1982**, *21*, 93.
- (25) Howes, K. R.; Pippin, C. G.; Sullivan, J. C.; Meisel, D.; Espenson, J. H.; Bakac, A. *Inorg. Chem.* **1988**, *27*, 2932.
- (26) Barigelletti, F.; De Cola, L.; Balzani, V.; Belsler, P.; von Zelewsky, A.; Vögtle, F.; Ebmeyer, F.; Grammenudi, S. *J. Am. Chem. Soc.* **1989**, *111*, 4662.
- (27) Billing, R. Z.; Benedix, R.; Stich, G.; Hennig, H. Z. *Anorg. Allg. Chem.* **1990**, *583*, 157.
- (28) Conrad, D. W.; Zhang, H.; Stewart, D. E.; Scott, R. A. *J. Am. Chem. Soc.* **1992**, *114*, 9909.
- (29) Nazarenko, A. Y.; Voloshin, Y. Z. *Zh. Anal. Khim.* **1982**, *37*, 1469.
- (30) Voloshin, Y. Z.; Kostromina, N. A.; Nazarenko, A. Y. *13th Int. Symp. Macrocycl. Chem. (Hamburg, 4–8 Sept, 1988)*. Book Abstr., Frankfurt/M.: S. a., 1988, 256.
- (31) Sakaguchi, U.; Tsuge, A.; Yoneda, H. *Inorg. Chem.* **1983**, *22*, 1630.
- (32) Miyoshi, K.; Izumoto, S.; Nakai, K.; Yoneda, H. *Inorg. Chem.* **1986**, *25*, 4654.

luminescent probes, and concentrators of luminescence.^{34–36} However, the high thermodynamic and kinetic stability displayed by the majority of such complexes,³⁷ together with metal ion encapsulation, sharply reduces the possibility of modification of clathrochelate frameworks of different types.

An apical functionalization of clathrochelates enables one to obtain complexes with improved chemical, physicochemical, biomimetic, and bioactive properties and characteristics that are primarily governed by functionalized groups. The mutual electronic influence of the apical substituents and the clathrochelate framework (and, therefore, the encapsulated ion) is negligible.³⁸ The steric effects of apical substituents are also small. The substituents in chelating (ribbed) fragments of polyenic clathrochelates have much greater steric and electronic effects on the polyhedron geometry and the central metal ion properties due to direct interaction of the π -system of a ligand and the π - and σ -system of a substituent. As a result, one has an opportunity to use such substituents in order to change the central metal ion characteristics, and, conversely, changing the central metal ion configuration via a redox transition and to affect the electronic characteristics of substituents. From this point of view, the synthesis of ribbed-functionalized clathrochelates with substituents apt to coordinate a metal ion to produce polynuclear complexes with interaction through the clathrochelate framework metal centers is of particular interest. The majority of macrobicyclic complexes have been obtained by a template condensation on a metal ion matrix. Ions of the essential biometals have proved to be the most efficient template agents in the synthesis of nitrogen-containing clathrochelates: a Co^{3+} ion in the case of polyanic clathrochelates (sepulchrates and sarcophagins) and a Fe^{2+} ion in the case of polyenic complexes (macrobicyclic tris-dioximates, tris-oximehydrazones, and tris-diiminates). Therefore, to work out the methods of synthesis for ribbed-functionalized tris-dioximate clathrochelates, we have chosen iron(II) complexes. The Fe^{2+} , Co^{3+} , and Ru^{2+} ions have isoelectronic configurations, and the procedures for the synthesis of functionalized complexes developed for iron(II) complexes can be extended to the formation of the corresponding cobalt(II,III) complexes and ruthenium(II) compounds, which are commonly used in different fields of biochemistry.³⁹ We reported earlier the first synthesis of a hexachloride precursor and that its reaction with thiophenol led to a functionalized complex.⁴⁰ We thought it was important to demonstrate that one could obtain ribbed-functionalized clathrochelates with substituents involving donor atoms different in nature, and exhibiting different electronic, spatial, and acidic–basic characteristics, which allowed us to directly improve coordination-chemical properties of such substituents and, consequently, also of a polynucleating clathrochelate complex.

Experimental Section

General Information. The reagents used, $\text{FeCl}_2 \cdot 4\text{H}_2\text{O}$, C_2CO_3 , K_2CO_3 , $\text{C}_6\text{H}_5\text{SH}$, CH_3SH , $\text{BF}_3 \cdot \text{O}(\text{C}_2\text{H}_5)_2$, sorbents, *n*-butyl- and phenylboronic acids, organic bases, and their salts, and organic solvents were obtained commercially (Fluka). Bis(2-(*o*-oxyphenoxy)diethyl ether was obtained as described in ref 41. The dichloroglyoxime (denoted as $\text{H}_2\text{-Cl}_2\text{Gm}$) was prepared by chlorination of glyoxime (H_2Gm) as described in ref 42.

The analyses for the carbon, hydrogen, and nitrogen content were carried out with a Carlo Erba model 1106 microanalyzer. Iron was determined spectrophotometrically.

To take FAB spectra, a high-resolution double-focusing MX-1310 (SEMI) mass spectrometer (electrostatic and magnetic sectors) was used. The substance to be investigated was dissolved in tricyanoethoxypropane. A sample of 5–10 mL of the solution was bombarded by an argon atom beam with an energy of 3.5 keV. The mass number scale in the mass spectrometer under FAB conditions was calibrated against the peaks of cluster ions. The analyzer peak resolution under FAB conditions was usually 10 000.

The relative intensities of the isotope peaks of molecular and fragment ions were calculated from the data on the abundance of natural isotopes of all the elements forming a part of these ions. The composition of molecular or fragment ions in the experimental mass spectra is confirmed by comparing the isotope peak series of these ions with the calculated ones.

The plasma desorption (PD) mass spectra were recorded in the positive spectral range on a time-of-flight biochemical BC MS (SEMI) mass spectrometer using an accelerating voltage of 20 kV. The ionization was induced by ^{252}Cf spontaneous decay fragments, and typically 20 000 decay acts have been registered. The samples (approximately 1–2 mg) were applied onto a gilded disk or onto a nitrocellulose layer.

The IR spectra of solid samples (KBr tablets) in the range 400–4000 cm^{-1} were recorded on a Specord M-80 spectrophotometer. The bands were assigned using the previous results. The UV–vis spectra of the solutions in chloroform in the range 230–800 nm were recorded on a Lambda 9 Perkin-Elmer spectrophotometer. The individual Gauss components of these spectra were calculated using the SPECTRA program. The ^1H , ^{13}C , and ^{11}B NMR spectra of the solutions in CDCl_3 were recorded on an AC-200 Bruker FT spectrometer.

^{57}Fe Mössbauer spectra were obtained on a YGRS-4M spectrometer with a constant acceleration mode. The spectra were collected on a 256-multichannel amplitude analyzer. The isomer shift was measured relative to sodium nitroprusside, and an α -Fe foil was used for the velocity scale calibration. ^{57}Co in Cr matrix was used as a source, which was always kept at room temperature. The minimal absorption line width in the spectrum of a standard sample of sodium nitroprusside was 0.24 mm/s.

Cyclic voltammograms were recorded in methylene dichloride and acetonitrile under an argon atmosphere and using a PI-50-1 potentiostat coupled with a B7-45 teraohmic potentiometer as a current voltage convertor. The scan rate was varied from 5 to 10 mV/s, which is close to the steady-state conditions for ultramicroelectrodes.^{43,44} Tetrabutylammonium tetrafluoroborate (0.1 M) was used as a supporting electrolyte. A platinum microelectrode 10 μm in diameter, thoroughly polished and rinsed before measurements, was chosen as a working electrode. A platinum wire was applied as an auxiliary electrode. A standard calomel reference electrode (SCE) was connected to the cell via a salt bridge. All potentials were referred to the redox potential of the ferrocene (Fc^+/Fc) couple as an internal standard. This potential is at +0.400 V vs SCE under the present experimental conditions.

Synthesis. Preparation of $\text{Fe}(\text{CH}_3\text{CN})_4\text{Cl}_2$ (1). $\text{FeCl}_2 \cdot 4\text{H}_2\text{O}$ (100 g, 0.5 mmol) was dissolved in acetonitrile (300 mL) with intensive stirring in a weak argon stream and heated to boiling, and 400 mL of

- (33) Izumoto, S.; Miyoshi, K.; Yoneda, H. *Bull. Chem. Soc. Jpn.* **1987**, *60*, 3199.
 (34) Alpha, B.; Balzani, V.; Lehn, J.-M.; Perathoner, S.; Sabbatini, N. *Angew. Chem., Int. Ed. Engl.* **1987**, *26*, 1266.
 (35) Blasse, G.; Dirksen, G. J.; Sabbatini, N.; Perathoner, S.; Lehn, J.-M.; Alpha, B. *J. Phys. Chem.* **1988**, *92*, 2419.
 (36) De Cola, L.; Barigelletti, F.; Balzani, V.; Belser, P.; von Zelewsky, A.; Vögtle, F.; Ebmeyer, F.; Grammenudi, S. *J. Am. Chem. Soc.* **1988**, *110*, 7210.
 (37) Voloshin, Y. Z.; Terekhova, M. I.; Noskov, Y. G.; Zavodnik, V. E.; Belsky, V. K. *An. Quim. Int. Ed.* **1998**, *94*, 142 and references therein.
 (38) Streletz, V. V.; Kukharenko, S. V.; Voloshin, Y. Z. *Pol. J. Chem.* **1995**, *69*, 1520.
 (39) Basile, L. A.; Barton, J. K. *J. Am. Chem. Soc.* **1987**, *109*, 7548 and references therein.
 (40) Voloshin, Y. Z.; Varzatskii, O. A.; Palchik, A. V.; Stash, A. I.; Belsky, V. K. *New J. Chem.* **1999**, *23*, 355.

- (41) Kyba, E. P.; Helgeson, R. C.; Maden, K.; Gokel, G. M.; Tarnowski, T. L.; Moore, S. S.; Cram, D. J. *J. Am. Chem. Soc.* **1977**, *99*, 2564.
 (42) Ponzio, G.; Baldracco, F. *Gazz. Chim. Ital.* **1930**, *60*, 415.
 (43) Bond, A. M.; Oldham, K. B.; Zoski, C. G. *J. Electroanal. Chem.* **1988**, *245*, 71.
 (44) Tait, R. J.; Bury, P. C.; Finin, B. C.; Reed, B. L.; Bond, A. M. *Anal. Chem.* **1993**, *65*, 3252.

water–acetonitrile azeotrope was distilled off. The microcrystalline product started to precipitate. The mixture was cooled to room temperature with stirring in an argon stream and filtered in the argon atmosphere. The solid was washed with toluene, and then hexane, and dried in vacuo at room temperature (yield: 126.6 g, 87%).

Preparation of $\text{Fe}(\text{Cl}_2\text{Gm})_3(\text{BC}_6\text{H}_5)_2$ (2). (The present paper offers a protocol of this complex preparation because we have reported earlier⁴⁰ only a general way of its synthesis.) Dichloroglyoxime (6.28 g, 40 mmol) and phenylboronic acid anhydride ($\text{C}_6\text{H}_5\text{BO}_3$) (2.27 g, 20 mmol), obtained by dehydration of phenylboronic acid at 130 °C, were suspended/dissolved in dry nitromethane (70 mL). $\text{Fe}(\text{CH}_3\text{CN})_4\text{Cl}_2$ (2.91 g, 10 mmol) was added in 10 portions to the boiling and stirring reaction mixture in the argon stream, and then 30 mL of nitromethane was distilled off and the mixture was cooled to room temperature. The microcrystalline orange solid was filtered, washed with hydrochloric acid (5 M, 20 mL), ethanol (10 mL), diethyl ether, and hexane, and dried in vacuo (yield: 6.26 g, 90%).

Elemental analysis, IR, UV–vis, NMR, and MS(PD) spectral data were presented in ref 40.

Preparation of $\text{Fe}(\text{Cl}_2\text{Gm})_3(\text{Bn}-\text{C}_4\text{H}_9)_2$ (3). This complex was synthesized like the previous one except that $n\text{-C}_4\text{H}_9\text{B}(\text{O}-n\text{-C}_4\text{H}_9)_2$ (4.08 g, 22 mmol) was used instead of $(\text{C}_6\text{H}_5\text{BO}_3)_3$ (yield: 5.12 g, 78%). Anal. Calcd for $\text{C}_{14}\text{H}_{18}\text{N}_6\text{O}_6\text{B}_2\text{Cl}_2\text{Fe}$: C, 25.59; H, 2.74; N, 12.80; Fe, 8.50. Found: C, 25.69; H, 2.75; N, 12.84; Fe, 8.49. MS(PD): m/z 656 (M^+), 533 ($\text{M} - \text{Cl}_2\text{C}_2\text{N}_2$)⁺. ¹H NMR (CDCl_3): δ (ppm) 0.72 (m, 4H, BCH_2), 0.93 (t, 6H, CH_3), 1.39 (m, 4H, CH_2), 1.41 (m, 4H, CH_2). ¹³C{¹H} NMR (CDCl_3): δ (ppm) 14.1 (s, CH_3), 16.0 (br s, BCH_2), 25.6 (s, CH_2), 25.8 (s, CH_2), 130.5 (s, $\text{C}=\text{N}$). IR (cm^{-1} , KBr): 1532 $\nu(\text{C}=\text{N})$, 893, 931 $\nu(\text{N}-\text{O})$, 1102 $\nu(\text{B}-\text{O})$. UV–vis (CHCl_3): λ_{max} ($10^{-3}\epsilon$) 259 (7.9), 285 (5.4), 313 (2.7), 423 (4.8), 453 (15) nm.

Preparation of $\text{Fe}(\text{Cl}_2\text{Gm})_3(\text{BF})_2$ (4). $\text{Fe}(\text{CH}_3\text{CN})_4\text{Cl}_2$ (1.45 g, 5 mmol), $\text{H}_2\text{Cl}_2\text{Gm}$ (3.14 g, 20 mmol), and $((n\text{-C}_4\text{H}_9)_4\text{N})\text{BF}_4$ (4 g) were suspended/dissolved in dry nitromethane (20 mL). Triethylamine (4.2 mL, 30 mmol) and $\text{BF}_3\cdot\text{O}(\text{C}_2\text{H}_5)_2$ (9.8 mL, 80 mmol) were added dropwise to the stirring reaction mixture in a weak argon stream for 30 min. The solution/suspension was boiled down to half volume, and $\text{BF}_3\cdot\text{O}(\text{C}_2\text{H}_5)_2$ (5 mL) was added. After intensive stirring for 1.5 h at 60 °C, the reaction mixture was deluted with a 3-fold volume of methanol and filtered. The orange solid was washed with water and then methanol, reprecipitated from hot chloroform with hexane, and dried in vacuo (yield: 1.83 g, 63%). Anal. Calcd for $\text{C}_6\text{N}_6\text{O}_6\text{B}_2\text{Cl}_2\text{F}_2\text{Fe}$: C, 12.41; N, 14.47; Fe, 9.61; Cl, 36.70. Found: C, 12.37; N, 14.45; Fe, 9.64; Cl, 36.74. MS(PD): m/z 580 (M^+), 457 ($\text{M} - \text{Cl}_2\text{C}_2\text{N}_2$)⁺. ¹³C{¹H} NMR (CDCl_3): δ (ppm) 132.8 (s, $\text{C}=\text{N}$). IR (cm^{-1} , KBr): 1546 $\nu(\text{C}=\text{N})$, 925, 957 $\nu(\text{N}-\text{O})$, 1171 $\nu(\text{B}-\text{O}) + \nu(\text{B}-\text{F})$. UV–vis (CHCl_3): λ_{max} ($10^{-3}\epsilon$) 264 (8.2), 354 (2.2), 422 (5.5), 451 (15) nm.

Preparation of $\text{Fe}(\text{C}_6\text{H}_5)_2\text{Gm}_3(\text{BC}_6\text{H}_5)_2$ (5). (The present paper offers a protocol of this complex preparation because we have reported earlier⁴⁰ only a general way of its synthesis.) The complex $\text{Fe}(\text{Cl}_2\text{Gm})_3(\text{BC}_6\text{H}_5)_2$ (0.5 g, 0.7 mmol) was dissolved in boiling dry 1,4-dioxane (50 mL), and an excess of thiophenol (0.6 mL, 6 mmol) and K_2CO_3 (2 g) were added to the solution. The reaction mixture was stirred for 8 h and filtered, and the filtrate was evaporated to 5 mL. The dark-red product was precipitated with ethanol, filtered, washed with ethanol, a small amount of diethyl ether, and then hexane, and dried in vacuo (yield: 1.83 g, 63%).

Elemental analysis, IR, UV–vis, NMR, and MS(FAB) spectral data were presented in ref 40.

Preparation of $\text{Fe}(\text{CH}_3\text{S})_2\text{Gm}_3(\text{BC}_6\text{H}_5)_2$ (6). $t\text{-C}_4\text{H}_9\text{OK}$ (1.61 g, 14 mmol) was suspended in dry THF (15 mL), the mixture was cooled to 0 °C, and excess methanethiol (1.5 mL, 26 mmol) was added. After intensive stirring for 10 min at 0 °C, the $\text{Fe}(\text{Cl}_2\text{Gm})_3(\text{BC}_6\text{H}_5)_2$ complex (1.4 g, 2 mmol) was added. The dark-red reaction mixture was stirred for 6 h at room temperature and refluxed for 4 h, and 5 mL of THF was distilled off. After cooling to room temperature, the mixture was filtered and the solid was washed with THF. Both filtrates were diluted with a 2-fold volume of methanol, heated to boiling, and treated with water (~15 mL). The oil-like product started to precipitate, and the mixture was left overnight at 0 °C. The solid was filtered and reprecipitated from saturated chloroform solution with hexane, washed with a small amount of diethyl ether and then hexane, and dried in

vacuo (yield: 1.03 g, 67%). Anal. Calcd for $\text{C}_{24}\text{H}_{28}\text{N}_6\text{O}_6\text{B}_2\text{FeS}_6$: C, 37.63; H, 3.66; N, 10.97; S, 25.08. Found: C, 37.64; H, 3.65; N, 11.08; Fe, 7.32; S, 25.12. MS(FAB): m/z 766 ($\text{M} + \text{H}^+$), 719 ($\text{M} + \text{H}^+ - \text{CH}_3\text{S}$)⁺, 672 ($\text{M} + \text{H}^+ - 2\text{CH}_3\text{S}$)⁺. MS(PD): m/z 765 (M^+), 718 ($\text{M} - \text{CH}_3\text{S}$)⁺. ¹H NMR (CDCl_3): δ (ppm) 2.75 (s, 18H, CH_3), 7.43 (m, 6H, Ph), 7.83 (m, 4H, Ph). ¹³C{¹H} NMR (CDCl_3): δ (ppm) 17.4 (s, CH_3), 127.4 (s, Ph), 127.8 (s, Ph), 131.4 (s, Ph), 140.0 (br s, BPh), 148.4 (s, $\text{C}=\text{N}$). IR (cm^{-1} , KBr): 1504 $\nu(\text{C}=\text{N})$, 898, 971 $\nu(\text{N}-\text{O})$, 1225 $\nu(\text{B}-\text{O})$. UV–vis (CHCl_3): λ_{max} ($10^{-3}\epsilon$) 272 (16), 310 (9.4), 399 (2.9), 498 (23) nm.

Preparation of $\text{Fe}(\text{C}_6\text{H}_5)_2\text{Gm}_3(\text{B}-n\text{-C}_4\text{H}_9)_2$ (7). Phenol (0.5 g, 6.3 mmol) was added to a solution of potassium methylate, obtained from metallic potassium (0.25 g, 6.3 mmol) with dry methanol (10 mL). The reaction mixture was evaporated to dryness, and the solid residue was left at 100 °C for 1 h in vacuo. The solution/suspension of the resulting potassium phenolate in dry THF (50 mL) was added to the solution of the complex $\text{Fe}(\text{Cl}_2\text{Gm})_3(\text{B}-n\text{-C}_4\text{H}_9)_2$ (0.66 g, 1 mmol) in THF (50 mL) at –20 °C. The reaction mixture was stirred for 1 h at this temperature and then for 8 h at room temperature and filtered. The filtrate was evaporated to dryness, and solid was washed with water and dissolved in chloroform. The chloroform solution was filtered through a Silasorb SPH-3000 layer and evaporated to dryness. The oil-like residue was treated with dry methanol, and solid obtained was dissolved in a chloroform/hexane mixture and filtered. The filtrate was evaporated to dryness, washed with hexane, and dried in vacuo (yield: 0.23 g, 23%). Anal. Calcd for $\text{C}_{50}\text{H}_{48}\text{N}_6\text{O}_{12}\text{B}_2\text{Fe}$: C, 59.92; H, 4.80; N, 8.39; Fe, 5.57. Found: C, 59.87; H, 4.93; N, 8.40; Fe, 5.61. MS(PD): m/z 1002 (M^+). ¹H NMR (CDCl_3): δ (ppm) 0.31 (m, 4H, BCH_2), 0.64 (t, 6H, CH_3), 0.86 (m, 4H, CH_2), 1.01 (m, 4H, CH_2), 6.91 (m, 12H, Ph), 7.18 (m, 6H, Ph), 7.31 (m, 12H, Ph). ¹³C{¹H} NMR (CDCl_3): δ (ppm) 13.9 (s, CH_3), 16.3 (br s, BCH_2), 25.4 (s, CH_2), 25.5 (s, CH_2), 116.8 (s, Ph), 124.6 (s, Ph), 129.6 (s, Ph), 143.5 (s, OPh), 154.7 (s, $\text{C}=\text{N}$). IR (cm^{-1} , KBr): 1584 $\nu(\text{C}=\text{N})$, 927, 988 $\nu(\text{N}-\text{O})$, 1096 $\nu(\text{B}-\text{O})$. UV–vis (CHCl_3): λ_{max} ($10^{-3}\epsilon$) 258 (36), 292 (9.0), 451 (35) nm.

Preparation of $\text{Fe}(\text{CwGm})_2(\text{Cl}_2\text{Gm})(\text{B}-n\text{-C}_4\text{H}_9)_2$ (8). Bis(2-(*o*-oxyphenoxy))diethyl ether (1.1 g, 3.8 mmol) was added to a solution of sodium methylate, obtained from metallic sodium (0.14 g, 6.3 mmol) with dry methanol (15 mL). The reaction mixture was refluxed for 30 min and evaporated to dryness, and solid residue was left at 90–100 °C for 1 h in vacuo. The resulting salt and interphase carrier $((n\text{-C}_4\text{H}_9)_4\text{N})\text{Cl}$ (0.45 g) were dissolved/suspended in dry THF (50 mL), and a solution of the complex $\text{Fe}(\text{Cl}_2\text{Gm})_3(\text{B}-n\text{-C}_4\text{H}_9)_2$ (1.0 g, 1.5 mmol) in THF (30 mL) was added dropwise to the stirring reaction mixture for 2 h. The solution/suspension was stirred for 5 h at 50 °C, cooled to room temperature, and filtered. The filtrate was evaporated to dryness. The solid was washed with water, then methanol, a small amount of diethyl ether, and hexane and dried in vacuo (yield: 0.60 g, 37%). Anal. Calcd for $\text{C}_{46}\text{H}_{50}\text{N}_6\text{O}_{16}\text{B}_2\text{Cl}_2\text{Fe}$: C, 50.62; H, 4.59; N, 7.70; Cl, 6.51; Fe, 5.12. Found: C, 50.52; H, 4.58; N, 7.59; Cl, 6.62; Fe, 5.02. MS(PD): m/z 1090 (M^+), 967 ($\text{M} - \text{Cl}_2\text{C}_2\text{N}_2$)⁺. ¹H NMR (CDCl_3): δ (ppm) –0.33 (m, 4H, BCH_2), 0.23 (m, 4H, CH_2), 0.61 (t, 6H, CH_3), 3.57 (m, 4H, OCH_2), 3.82 (m, 4H, OCH_2), 4.04 (m, 8H, OCH_2), 6.09 (m, 8H, Ph), 7.09 (m, 8H, Ph). ¹³C{¹H} NMR (CDCl_3): δ (ppm) 14.0 (s, CH_3), 16.2 (br s, BCH_2), 25.0 (s, CH_2), 25.4 (s, CH_2), 67.0 (s, OCH_2), 69.7 (s, OCH_2), 111.6 (s, Ph), 119.1 (s, Ph), 120.3 (s, Ph), 125.4 (s, Ph), 143.9 (s, OPh), 148.9 (s, OPh), 125.1 (s, $\text{C}=\text{N}$), 140.5 (s, $\text{OC}=\text{N}$). IR (cm^{-1} , KBr): 1573 $\nu(\text{C}=\text{N})$, 912, 997 $\nu(\text{N}-\text{O})$, 1110 $\nu(\text{B}-\text{O})$. UV–vis (CHCl_3): λ_{max} ($10^{-3}\epsilon$) 265 (13), 277 (3.5), 326 (4.2), 417 (7.3), 469 (4.0), 497 (5.1) nm.

Preparation of $\text{Fe}(\text{CwGm})_3(\text{B}-n\text{-C}_4\text{H}_9)_2$ (9). The complex was synthesized like the previous one except that an excess of the disodium salt of bis(2-(*o*-oxyphenoxy))diethyl ether, obtained from metallic sodium (0.25 g, 10.8 mmol) and bis(2-(*o*-oxyphenoxy))diethyl ether (2.0 g, 6.9 mmol), was used and reaction time was 30 h.

The reaction mixture was filtered, and filtrate was precipitated with a 3-fold volume of hexane. The precipitate was filtered, and filtrate was evaporated to dryness. The solid was washed with water and then methanol, and the product was extracted with diethyl ether. The extract was evaporated to dryness, and the resulting orange solid was washed with hexane and dried in vacuo (yield: 0.45 g, 23%). Anal. Calcd for $\text{C}_{62}\text{H}_{66}\text{N}_6\text{O}_{21}\text{B}_2\text{Fe}$: C, 56.91; H, 5.05; N, 6.42; Fe, 4.27. Found: C,

Table 1. Crystallographic Data and Experimental Details for Fe(Cl₂Gm)₃(B-*n*-C₄H₉)₂ (**3**), Fe(Cl₂Gm)₃(BF)₂·2THF (**4**), Fe((CH₃S)2Gm)₃(BC₆H₅)₂·THF (**6**), Fe((C₆H₅O)2Gm)₃(B-*n*-C₄H₉)₂ (**7**), and Fe((*n*-C₄H₉NH)2Gm)₂(Cl₂Gm)(BC₆H₅)₂ (**11**)

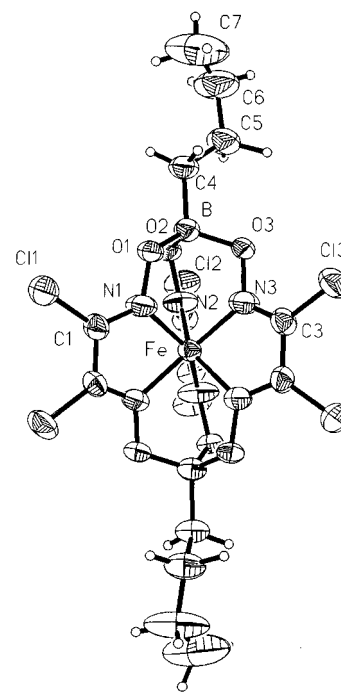
	3	4	6	7	11
empirical formula	C ₁₄ H ₁₈ B ₂ C ₁₆ FeN ₆ O ₆	C ₁₄ H ₁₆ B ₂ C ₁₆ FeN ₆ O ₈	C ₂₈ H ₃₆ B ₂ FeN ₆ O ₇ S ₆	C ₅₀ H ₄₈ B ₂ FeN ₆ O ₁₂	C ₃₄ H ₅₀ B ₂ Cl ₂ FeN ₁₀ O ₆
fw	656.51	724.52	838.46	1002.42	843.21
color, habit	orange, prism	orange, prism	dark red, prism	brown, prism	red, prism
cryst dimens, mm	0.35 × 0.20 × 0.06	0.42 × 0.40 × 0.37	0.42 × 0.98 × 0.26	0.42 × 0.36 × 0.24	0.95 × 0.45 × 0.45
<i>a</i> , Å	25.075(5)	17.634(4)	14.379(3)	17.718(4)	37.783(8)
<i>b</i> , Å	8.135(2)	8.197(2)	14.470(3)	25.075(5)	17.227(3)
<i>c</i> , Å	16.415(3)	18.799(4)	18.003(4)	13.445(5)	24.285(5)
β , deg	130.53(3)	92.62(3)		120.86(3)	120.48(3)
<i>V</i> , Å ³	2545.0(9)	2715(1)	3746(1)	5128(2)	13622(5)
<i>Z</i>	4	4	4	4	12
cryst syst	monoclinic	monoclinic	orthorhombic	monoclinic	monoclinic
space group	<i>C2/c</i>	<i>C2/c</i>	<i>Pccn</i>	<i>C2/c</i>	<i>C2/c</i>
<i>D</i> _{calc} , g cm ⁻³	1.713	1.763	1.487	1.298	1.233
μ , mm ⁻¹	1.266	1.208	0.789	0.360	0.500
data/restraints/params	1728/0/187	1582/0/196	1344/0/226	2699/0/417	4956/0/745
weighting scheme	1/[$\sigma^2(F_o^2)$ + (0.0522 <i>P</i>) ² + 8.99 <i>P</i>], <i>P</i> = (<i>F</i> _o ² + 2 <i>F</i> _c ²)/3	1/[$\sigma^2(F_o^2)$ + (0.113 <i>P</i>) ² + 10.96 <i>P</i>], <i>P</i> = (<i>F</i> _o ² + 2 <i>F</i> _c ²)/3	1/[$\sigma^2(F_o^2)$ + (0.054 <i>P</i>) ² + 3.426 <i>P</i>], <i>P</i> = (<i>F</i> _o ² + 2 <i>F</i> _c ²)/3	1/[$\sigma^2(F_o^2)$ + (0.1004 <i>P</i>) ² + 4.2227 <i>P</i>], <i>P</i> = (<i>F</i> _o ² + 2 <i>F</i> _c ²)/3	1/[$\sigma^2(F_o^2)$ + (0.12 <i>P</i>) ² + 19.50 <i>P</i>], <i>P</i> = (<i>F</i> _o ² + 2 <i>F</i> _c ²)/3
<i>R</i> , %	0.0379	0.0639	0.0289	0.0458	0.0492
<i>R</i> _w , %	0.1007	0.1738	0.0803	0.1227	0.1447
<i>F</i> (000)	1320	1440	1736	2088	5304
GOF ^c	1.039	1.116	0.875	1.061	1.095

$$^a R = (\sum |F_o| - |F_c|) / \sum |F_o|. \quad ^b R_w = [(\sum w|F_o| - |F_c|) / \sum w|F_o|]^{1/2}. \quad ^c \text{GOF} = [(\sum w|F_o| - |F_c|)^2 / (N_{\text{obs}} - N_{\text{param}})]^{1/2}.$$

56.81; H, 5.10; N, 6.55; Fe, 4.34. MS(PD): *m/z* 1307 (M)⁺. ¹H NMR (CDCl₃): δ (ppm) -0.30 (m, 4H, BCH₂), 0.25 (m, 4H, CH₂), 0.51 (t, 6H, CH₃), 0.78 (m, 4H, CH₂), 3.91 (m, 12H, OCH₂), 4.07 (m, 12H, OCH₂), 6.79 (m, 12H, Ph), 6.99 (m, 12H, Ph). ¹³C{¹H} NMR (CDCl₃): δ (ppm) 14.0 (s, CH₃), 16.2 (br s, BCH₂), 24.8 (s, CH₂), 25.5 (s, CH₂), 67.5 (s, OCH₂), 70.0 (s, OCH₂), 112.2 (s, Ph), 118.7 (s, Ph), 120.2 (s, Ph), 125.0 (s, Ph), 144.2 (s, OPh), 149.0 (s, OPh), 139.6 (s, OC=N). IR (cm⁻¹, KBr): 1563 ν (C=N), 931, 992 ν (N-O), 1112 ν (B-O). UV-vis (CHCl₃): λ_{max} (10⁻³ε) 246 (16), 259 (6.9), 278 (16), 449 (14) nm.

Preparation of Fe((12anS₄Gm)₃(BC₆H₅)₂ (10**).** Cs₂CO₃ (3.2 g) and 3,5-dithiaoctane-1,8-dithiol (0.8 g, 3.7 mmol) were suspended/dissolved in dry DMF (15 mL), stirred for 30 min in the argon stream, and cooled to -20 °C. The complex Fe(Cl₂Gm)₃(BC₆H₅)₂ (0.7 g, 1 mmol) was added, and the reaction mixture was stirred for 3 h at -20 °C and for 3 h at room temperature. The mixture was left overnight, stirred for 6 h at 60 °C, diluted with saturated Na₂SO₄ aqueous solution, and filtered. The solid was washed with methanol, extracted with chloroform, and precipitated from chloroform solution with hexane. The resulting red solid was separated by chromatography on Silasorb SPH-300 (eluent: CHCl₃), and the major dark-red product was isolated, washed with a small amount of diethyl ether and then hexane, and dried in vacuo (yield: 0.03 g, 2.7%). Anal. Calcd for C₃₆H₄₆N₆O₆S₁₂B₂Fe: C, 38.56; H, 4.11; N, 7.50; Fe, 4.89. Found: C, 38.41; H, 4.18; N, 7.41; Fe, 4.98. MS(PD): *m/z* 1120 (M)⁺. ¹H NMR (CDCl₃): δ (ppm) 2.3–2.8 (m, 36H, CH₂), 7.43 (m, 6H, Ph), 7.81 (m, 4H, Ph). ¹³C{¹H} NMR (CDCl₃): δ (ppm) 32.4 (s, SCH₂), 33.3 (s, SCH₂), 34.2 (s, SCH₂), 127.8 (s, Ph), 128.4 (s, Ph), 131.4 (s, Ph), 139.2 (br s, BPh), 149.0 (s, C=N). IR (cm⁻¹, KBr): 1500 ν (C=N), 897, 973 ν (N-O), 1227 ν (B-O). UV-vis (CHCl₃): λ_{max} (10⁻³ε) 274 (13), 310 (7.9), 428 (3.3), 504 (16) nm.

Preparation of Fe((*n*-C₄H₉NH)2Gm)₂(Cl₂Gm)(BC₆H₅)₂ (11**).** The complex Fe(Cl₂Gm)₃(BC₆H₅)₂ (0.35 g, 0.5 mmol) was dissolved in dry DMF (15 mL) and an excess of *n*-butylamine (0.45 mL, 4.5 mmol) was added. The reaction mixture was stirred for 30 h, and the resulting red-violet solution was precipitated with a 5-fold volume of water. The solid was filtered, dried in vacuo, and reprecipitated from saturated chloroform solution with methanol (yield: 0.13 g, 31%). Anal. Calcd for C₃₄H₅₀N₁₀O₆B₂Cl₂Fe: C, 48.39; H, 5.93; N, 16.60; Fe, 6.62; Cl, 8.42. Found: C, 48.51; H, 5.97; N, 16.55; Fe, 6.71; Cl, 8.38. MS(PD): *m/z* 843 (M)⁺, 720 (M - Cl₂C₂N₂)⁺. ¹H NMR (CDCl₃): δ (ppm) 0.93 (t, 12H, CH₃), 1.46 (m, 16H, CH₂CH₂), 3.36 (m, 8H, NCH₂), 5.58 (br s, 4H, NH), 7.45 (m, 6H, Ph), 7.88 (m, 4H, Ph). ¹³C{¹H} NMR (CDCl₃): δ (ppm) 13.6 (s, CH₃), 19.2 (s, CH₂), 33.5 (s, CH₂), 44.5 (s, NCH₂), 127.3 (s, Ph), 127.6 (s, Ph), 131.5 (s, Ph), 141.7 (br s, BPh), 126.4 (s, ClC=N), 151.3 (s, NC=N). IR (cm⁻¹, KBr): 1527, 1585 ν (C=N), 904, 962 ν (N-O), 1231 ν (B-O). UV-vis (CHCl₃): λ_{max} (10⁻³ε) 252 (21), 302 (6.8), 360 (5.5), 425 (7.5), 490 (7.0), 543 (6.5) nm.

**Figure 1.** Molecular structure of Fe(Cl₂Gm)₃(B-*n*-C₄H₉)₂ (**3**). Thermal ellipsoids are drawn at the 50% probability level.

X-ray Crystallography. The details of crystal data collection and parameters refinement for Fe(Cl₂Gm)₃(B-*n*-C₄H₉)₂ (**3**), Fe(Cl₂Gm)₃(BF)₂·2THF (**4**), Fe((CH₃S)2Gm)₃(BC₆H₅)₂·THF (**6**), Fe((C₆H₅O)2Gm)₃(B-*n*-C₄H₉)₂ (**7**), and Fe((*n*-C₄H₉NH)2Gm)₂(Cl₂Gm)(BC₆H₅)₂ (**11**) are listed in Table 1. Single crystals of these complexes were grown from acetone/water (**3**), THF (**4** and **6**), benzene/*iso*-octane (**7**), and pentane (**11**) at room temperature. Data were collected at 293 K on a CAD4 diffractometer using Mo K α (β -filtered) radiation (λ = 0.710 73 Å) with $\theta/2\theta$ scans. The structures were solved by the heavy-atom method, and refinements were done by full-matrix least squares on *F*² for all data with anisotropic thermal parameters for non-hydrogen atoms and isotropic for hydrogen ones. All oxygen atoms in structure **3** (Figure 1) are statistically disordered by two positions with occupation 2:1. The THF molecules in structures **4** and **6** are partially disordered. The molecules of **3**, **4**, **6**, and **7** are located on a 2-fold axis in crystals. For complex **11** (Figure 2) two types of molecules (in general position, type A, and located on a second-order axis, type B) with occupation 2:1 were elucidated in the unit cell. All calculations were made using the SHELXTL-93 program package.⁴⁵

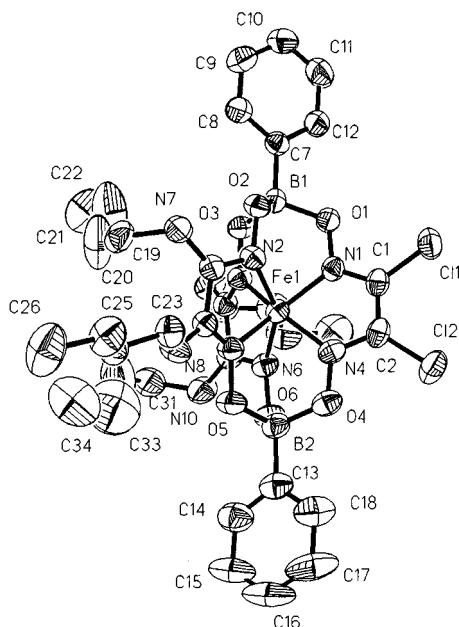


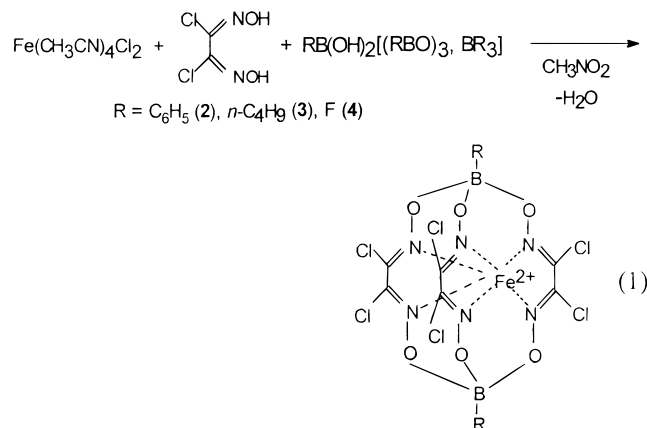
Figure 2. Molecular structure of $\text{Fe}((n\text{-C}_4\text{H}_9\text{NH})_2\text{Gm})(\text{Cl}_2\text{Gm})\text{-}(\text{BC}_6\text{H}_5)_2$ (**11**). Hydrogen atoms are omitted for clarity. Thermal ellipsoids are drawn at the 50% probability level.

Results and Discussion

Synthesis of Precursors. The most feasible routes for the synthesis of ribbed-functionalized α -dioximate clathrochelates (I–III) are shown in Scheme 1. It should be noted that halogen–carbon bonds are reasonably active in nucleophilic substitution reactions. Their dihalogenoxime complexes are relatively stable, and, unlike dihalogenoximes, they are available and undergo no intramolecular conversions that could complicate modification reactions. It is rather complicated to use the preliminarily functionalized α -dioximes (route I) in the synthesis of clathrochelates to obtain partially substituted compounds and complexes with redox-active coordinating groups. In addition, the preliminarily functionalized α -dioximes in the course of a template condensation on the metal ion can react not only with oxime groups but also with functionalizing substituents. Side reactions of these groups can markedly reduce the yield of the desired products and hinder their isolation.⁴⁶ Consequently, routes II and III (Scheme 1) were chosen for the synthesis of the ribbed-functionalized clathrochelates. Route II was regarded as the most promising procedure since new methods for the synthesis of the starting glyoximate clathrochelates with yields of 70–80% were developed. However, we failed to implement a complete halogenation of dioximate fragments of such complexes and to isolate hexahalogenide precursors of triribbed-functionalized clathrochelates. A mixture of partial substitution products, largely containing trihalogen-substituted compounds, was obtained. In addition, in the case of a phenylboronic $\text{FeGm}_3\text{-}(\text{BC}_6\text{H}_5)_2$ glyoximate, side halogenation reactions of aromatic substituents at apical boron atoms were observed.

The use of route III presented problems since our attempts to obtain hexahalogenide precursors from preliminarily prepared dihalogendioximes by the recently developed methods of synthesis of such clathrochelates⁴⁷ were not successful. Nevertheless, we still managed to select conditions under which the yield of these complexes was 60–90%: nitromethane was

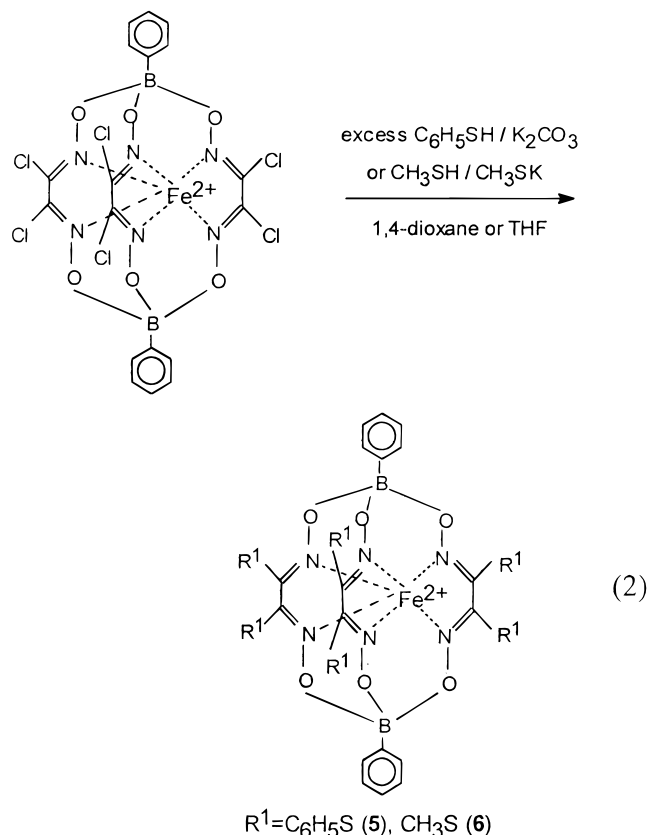
used as a solvent and acetonitrile solvate $\text{Fe}(\text{CH}_3\text{CN})_4\text{Cl}_2$ (**1**) as a source of Fe^{2+} ions, and the water was removed from the reaction mixture (reaction 1). The three hexachloride precursors with phenylboronic (**2**), *n*-butylboronic (**3**), and fluoroboronic (**4**) capping groups were obtained.



The compounds obtained were stable in an acid medium; however, in an alkaline medium chlorine atoms have been replaced by OH groups with the subsequent destruction and formation of plane-square bis-complexes. The traces of water should be removed from all reactants and solvents. So far we have failed to obtain the corresponding ribbed-functionalized clathrochelates through the interaction of precursors with $\text{KP}(\text{C}_6\text{H}_5)_2$, $\text{Na}(\text{cp})$, and NaNH_2 because of their high basicity and destruction of clathrochelates.

Reactions of Precursors with Aryl and Alkyl Thiolates.

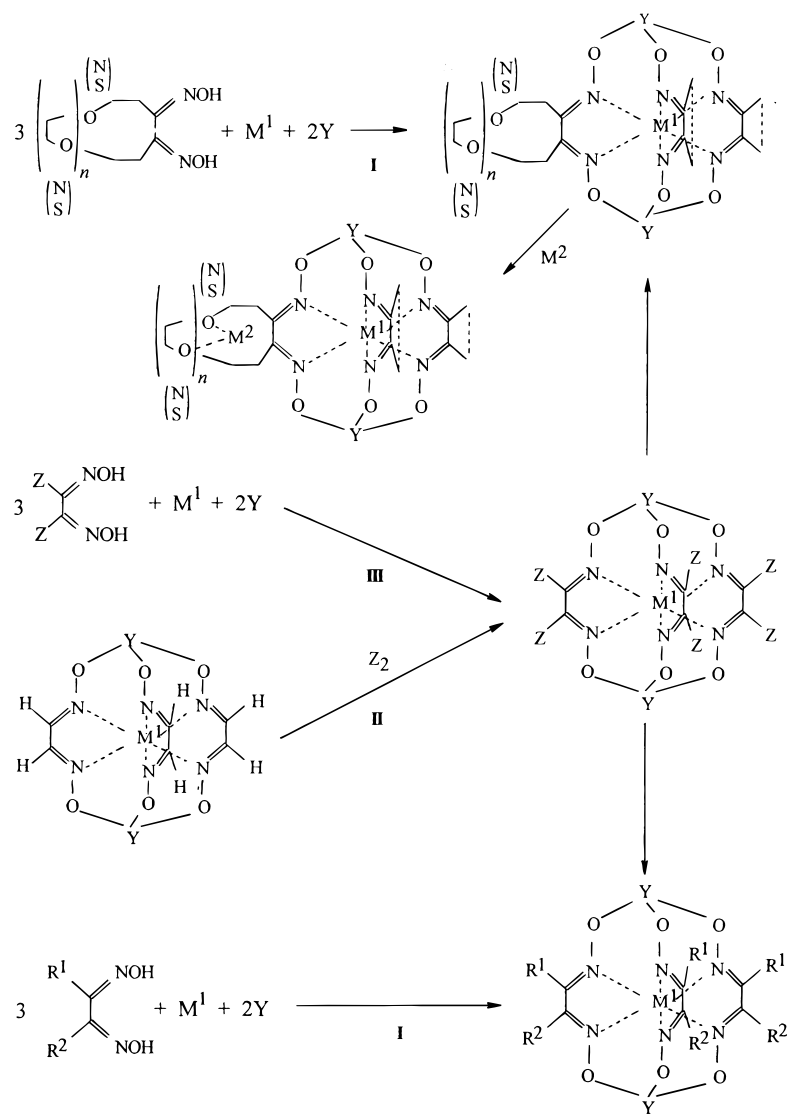
Hexachloride precursors have interacted with excess thiophenol in the presence of potassium carbonate under soft conditions to yield hexathiophenolic clathrochelates (reaction 2).



(45) Sheldrick, G. M. *SHELXTL-93 programs for Structure Refinement*; University of Göttingen: Göttingen, Germany, 1993.

(46) Voloshin, Y. Z.; Varzatskii, O. A. Unpublished results.

Scheme 1



$R^1, R^2 = PAIk_2(Ar_2), NHAIk(Ar), NAIk_2(Ar_2)$, crown ether,
ferrocenyl, $SAIk(Ar)$, cp, CN, $OAlk(Ar)$, $PO(OH)_2$
Y = Lewis acid, M = metal ion, Z = halogen

The reaction with an excess of methylmercaptan in the presence of potassium carbonate at room temperature allowed us to obtain partially substituted products only, mainly trisubstituted clathrochelates. The formation of such complexes dominates in the case of partial substitution. The heating of the reaction mixture led to no improvement in the results because of a low boiling point and a high volatility of CH_3SH . Therefore, a more active potassium derivative, CH_3SK , was used in the synthesis of the hexasubstituted product. In this case, the reaction readily proceeded in a high yield.

The thioalkyl-containing macrobicyclic complexes have been dealkylated and realkylated easily under action of potassium thiolates in aprotic media (the products of de- and realkylation reactions were detected by PD and FAB mass spectrometry). In this respect the thioalkyl-containing clathrochelates are close to the aryl alkyl sulfides.⁴⁸ In the

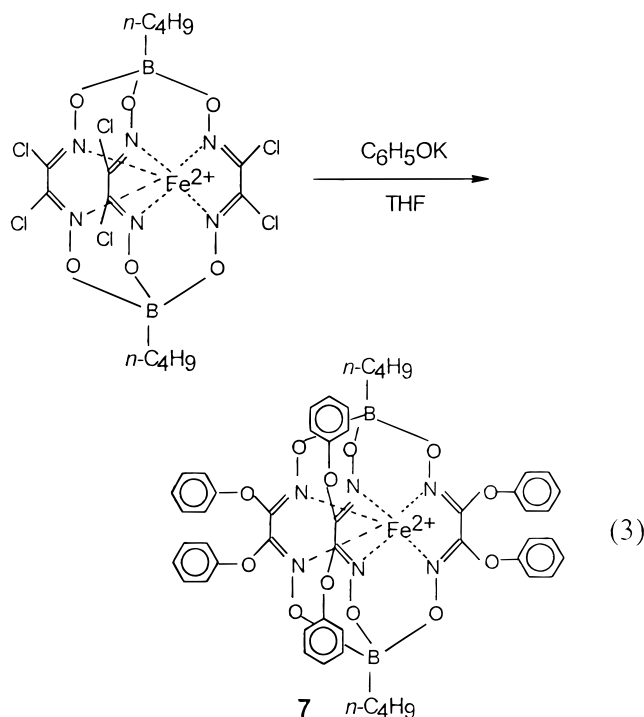
course of thioalkyl derivative synthesis with an excess of potassium thiolate, a mixture of dealkylated products was obtained in addition to the desired hexathioalkyl clathrochelates. As a result, the yield of the latter complexes was usually no more than 70%. The addition of the corresponding alkyl iodide and potassium carbonate to the reaction mixture in the final stage of reaction leads to an increase in yields to 95% by alkylation of HS groups, resulting in the side dealkylation process.

Reactions of Precursors with Phenolate and Alcohates.

The reaction of *n*-butylboronic precursor **3** with potassium phenolate led to formation of the hexaphenolate complex $Fe((C_6H_5O)_2Gm)_3(B-n-C_4H_9)_2$ (reaction 3). Unfortunately, we have failed to synthesize the *n*- and *tert*-butoxy-containing clathrochelates because of destruction of starting precursors.

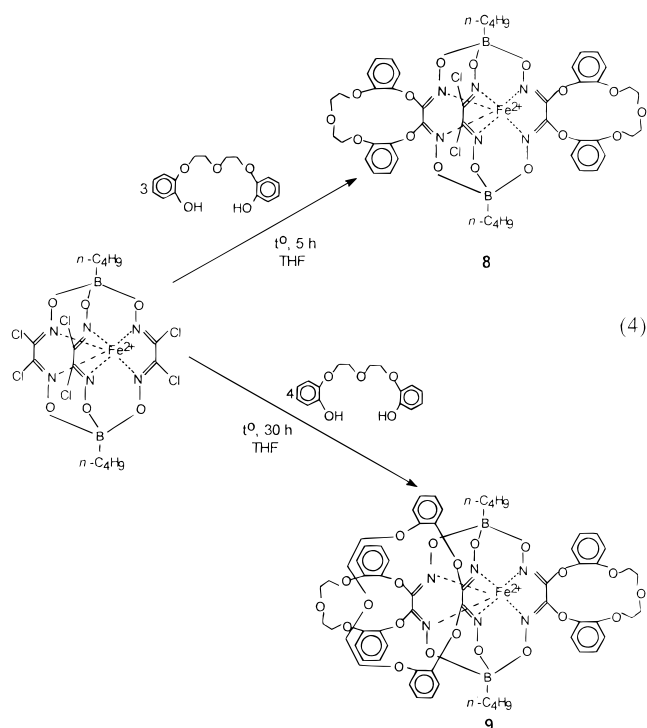
(47) Voloshin, Y. Z.; Kostromina, N. A.; Nazarenko, A. Y. *Inorg. Chim. Acta* **1990**, *170*, 181 and references therein.

(48) Testaferri, L.; Tiecco, M.; Tingoli, N.; Chianeli, D.; Montanucci, M. *Synthesis* **1983**, 751.



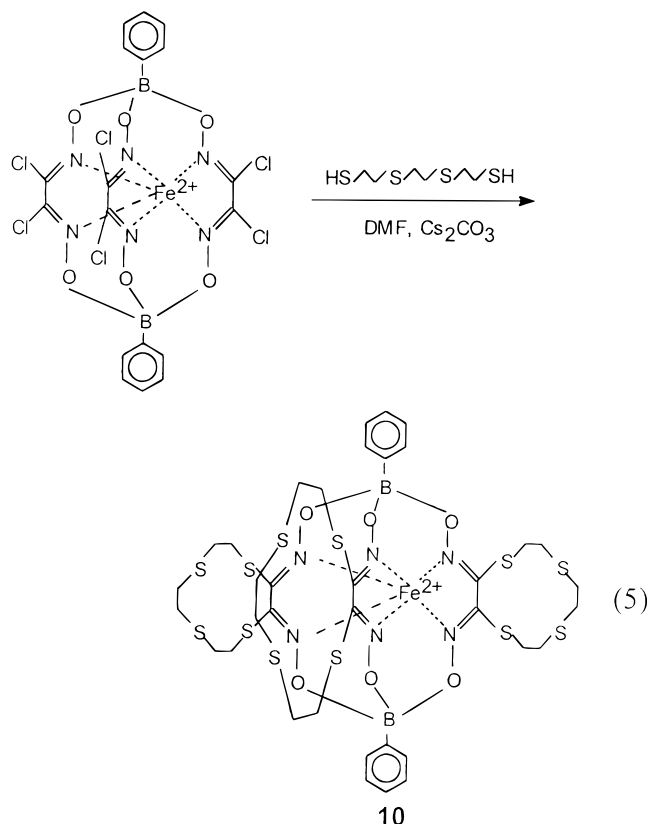
Synthesis of Oxo- and Thioether Crown Clathrochelates.

The well-known synthetic procedures for crown ethers and their analogues^{49–51} allowed us to synthesize clathrochelates with dioximate fragments of the oxo- and thioether crown type (reactions 4 and 5). The interaction of phenylboronic (**2**) and *n*-butylboronic (**3**) precursors with 3 mol of the sodium salt of bis(2-(*o*-oxyphenoxy))diethyl ether for 5 h in THF at 50–60 °C led largely to the formation of asymmetrical two-ribbed-substituted products that seemed to be promising for a further modification with more active agents. The reactions of **3** were studied in more detail. A 30% excess of the sodium salt of bis(2-(*o*-oxyphenoxy))diethyl ether and an increase in the reaction time up to 30 h permitted us to isolate a tricrown etheric clathrochelate (reaction 4). Tetrabutylammonium salt ((*n*-



(C_4H_9)₄N)Cl) was used as an interphase catalyst for the condensation reaction. The side products of this reaction mainly resulted from the condensation one of the two deprotonated oxy groups of bis(2-(*o*-oxyphenoxy))diethyl ether and the dichloroglyoximate fragments of the precursor. Such open-chain compounds are readily soluble in methanol. An attempt to use the sodium triflate at a high concentration and to create the appropriate conditions for a template condensation on the sodium ion through orientation of the terminal oxygen atoms met with failure.

The template condensation of **2** with 3,5-dithiaoctane-1,8-dithiol in the presence of Cs_2CO_3 allowed us to obtain tris(12anS₄)-containing clathrochelate **10** in a low yield. The resultant clathrochelate is a representative of a promising series of models of “blue” proteins.



Unfortunately, we did not succeed in selecting the appropriate conditions for the synthesis of tris-azamacrocyclic clathrochelates containing dioximate fragments in polyazamacrocyclic rings. The attempts to use open-chain polyamines, as well as their complexes with transition metals, primarily Ni^{2+} , gave no desired results.

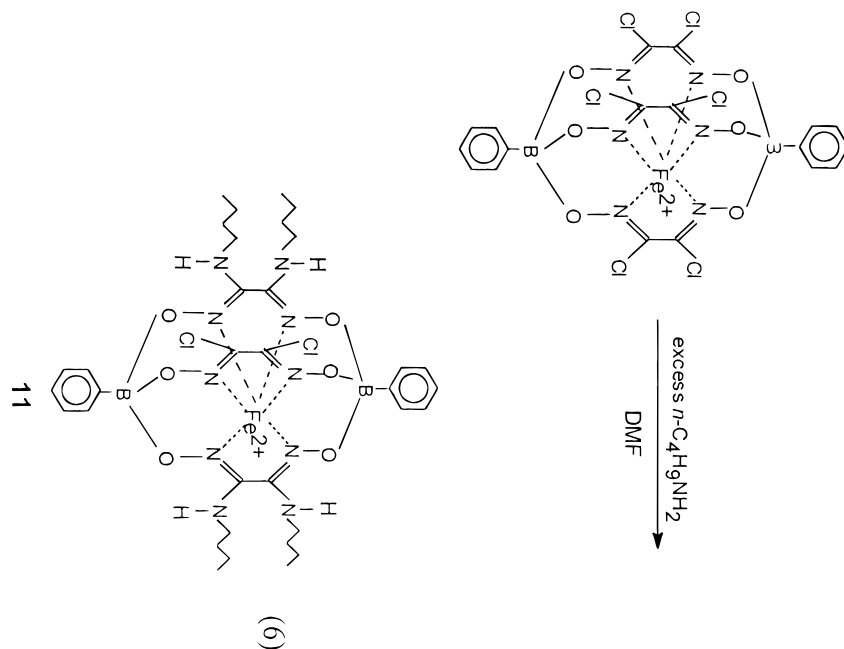
Reactions of Precursors with Aliphatic and Aromatic Amines. The reaction of a phenylboronic precursor **2** with an excess of *n*-butylamine unexpectedly led to preferential formation of the tetrasubstituted clathrochelate by the modification of two of the three dichloroglyoximate fragments (reaction 6). A similar product was obtained also in the case of cyclohexylamine. The attempts to obtain a hexa-*n*-butylaminic clathro-

(49) Gokel, G. W.; Korzeniowski, S. H. *Macrocyclic Polyether Syntheses*; Springer: Berlin, 1982.

(50) *Synthesis of Macrocycles. The Design of Selective Complexing Agents*; Izatt, R. M., Christensen, J. J., Eds.; Wiley-Interscience: New York, 1987.

(51) *Macrocyclic Synthesis. A Practical Approach*; Parker, D., Ed.; Oxford University Press: Oxford, 1996.

chelate were not successful. At the same time, the interaction of the tetrasubstituted product with more active agents, such as CH₃SK or C₆H₅SK, is expected to lead to the formation of the corresponding asymmetrical ribbed-functionalized clathrochelates. The interaction of precursors **2** and **3** with aniline and its derivatives under conditions that varied over a wide range resulted in the formation of di- and trisubstituted products, which failed to be isolated as individual compounds.



Structure and Spectra. The X-ray data summary is presented in Table 2. The fact that the geometry of the coordination polyhedron of the precursors changed depending on the nature of a substituent on the boron atom attracted attention first. In the phenylboronic complex, the distortion angle φ (Scheme 2), describing a change from a trigonal-prismatic ($\varphi = 0^\circ$) environment to near regular octahedral ($\varphi = 60^\circ$) one, is the smallest of all those known for macrobicyclic tris-dioximate complexes,⁵³ whereas for the *n*-butylboronic **3** and fluoroboronic **4** precursors, the magnitude of φ is close to that most common for boron-containing clathrochelates. Functionalized complexes **5**, **6**, **7**, and **11** exhibited a geometry with still greater octahedral distortion. In this case, the Fe–N distances and the bite angle α remained practically unchanged. However, there was a rather significant decrease (approximately 0.06–0.09 Å) in the distance *h* between the coordination polyhedron bases (Scheme 2): the change in *h* is a consequence of the constancy of Fe–N bond lengths as φ increased. Thus, the change in the coordination polyhedron on passing from trigonal-prismatic to near regular octahedral geometry may be described as a rotary-translational contraction along the C₃ symmetry axis that passed through the

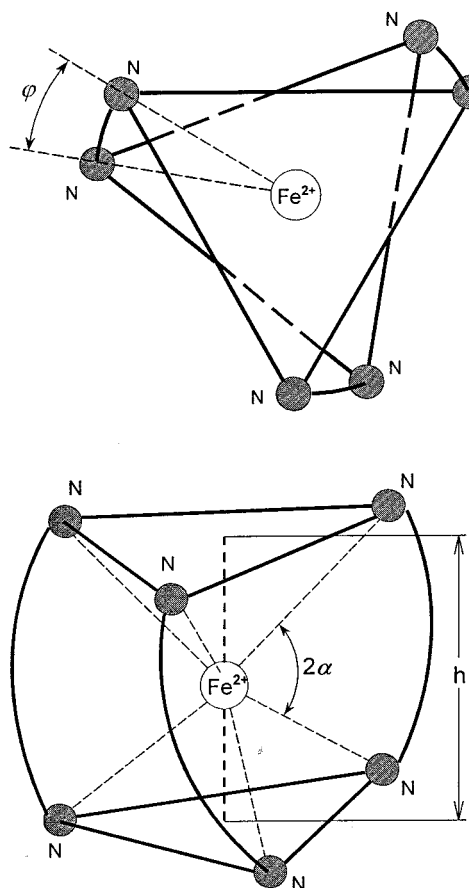
- (52) Lindeman, S. V.; Struchkov, Y. T.; Voloshin, Y. Z. *Pol. J. Chem.* **1993**, *67*, 1575.
 (53) Voloshin, Y. Z.; Kron, T. E.; Belsky, V. K.; Zavadnik, V. E.; Malesin, Y. A.; Kozachkov, S. G. *J. Organomet. Chem.* **1997**, *536/537*, 207 and references therein.

Table 2. Parameters of ⁵⁷Fe Mössbauer Spectra (mm/s) and the Main X-ray Data for Hexachloride Clathrochelate Precursors and Their Derivatives

compound	IS	QS	φ , deg	Fe–N, ^a Å	<i>h</i> , ^b Å	α , ^c deg	C–C, ^a Å	C=N, ^a Å	C–C=N, ^a deg	N–O, ^d Å	N–O–B, ^d deg	B–O, ^d Å	O–B–C ^d (O–B–F), deg	O–B–O, ^d deg	Δ , ^e Å	N=C–C=N, ^f deg
Fe(Cl ₂ Gm) ₃ (BC ₆ H ₅) ₂ ⁴⁰	0.39	0.68	5.4	1.90	2.39	39.0	1.418	1.274	112.6	1.363	110.2	1.510	110.8	108.2	0.009	0.9
Fe(Cl ₂ Gm) ₃ (B- <i>n</i> -C ₄ H ₉) ₂	0.37	0.62	16.1	1.90	2.38	39.1	1.422	1.285	112.4	1.376	111.1	1.504	109.8	109.2	0.089	8.6
Fe(Cl ₂ Gm) ₃ (BF) ₂ ·2THF	0.37	0.64	17.1	1.91	2.36	39.0	1.429	1.276	112.3	1.370	112.1	1.464	108.0	110.9	0.083	8.1
Fe((C ₆ H ₅ O)2Gm) ₃ (B- <i>n</i> -C ₄ H ₉) ₂	0.41	0.52	25.2	1.91	2.36	39.8	1.440	1.296	112.8	1.372	112.9	1.502	109.5	109.5	0.096	9.2
Fe((CH ₃ S)2Gm) ₃ (BC ₆ H ₅) ₂ ·THF	0.36	0.29	25.3	1.91	2.32	39.3	1.461	1.298	111.3	1.377	112.2	1.491	109.7	110.2	0.115	10.9
Fe((C ₆ H ₅)2Gm) ₃ (BC ₆ H ₅) ₂ ⁴⁰	0.34	0.25	25.6	1.91	2.33	39.5	1.452	1.302	111.8	1.364	113.2	1.426	109.4	109.6	0.128	11.3
Fe(<i>n</i> -C ₄ H ₉ NH)2Gm) ₂ (Cl ₂ Gm)(BC ₆ H ₅) ₂ (type A)	0.38	0.69	27.3	1.92	2.33	39.5	1.427	1.362	111.5	1.362	112.8	1.500	108.7	110.2	0.102	9.8
				1.89	40.3		(Cl ₂ Gm)	(Cl ₂ Gm)		(Cl ₂ Gm)					(Cl ₂ Gm)	(Cl ₂ Gm)
				(Cl ₂ Gm)	(Cl ₂ Gm)		1.458	1.305		1.396					0.282	26.8
				1.96	39.0		(N ₂ Gm)	(N ₂ Gm)		(N ₂ Gm)					0.206	19.4
				(N ₂ Gm)	(N ₂ Gm)										(N ₂ Gm)	(N ₂ Gm)
Fe(<i>n</i> -C ₄ H ₉ NH)2Gm) ₂ (Cl ₂ Gm)(BC ₆ H ₅) ₂ (type B)	0.38	0.69	29.2	1.91	2.30	39.5	1.435	1.304	111.3	1.367	112.1	1.490	108.4	110.7	0.105	10.0
				1.89	40.4		(Cl ₂ Gm)	(Cl ₂ Gm)		(Cl ₂ Gm)					(Cl ₂ Gm)	(Cl ₂ Gm)
				(Cl ₂ Gm)	(Cl ₂ Gm)		1.476	1.291		1.400					0.203	19.2
				1.93	39.0		(N ₂ Gm)	(N ₂ Gm)		(N ₂ Gm)					0.206	19.6
				(N ₂ Gm)	(N ₂ Gm)										(N ₂ Gm)	(N ₂ Gm)
FeGm ₃ (B- <i>n</i> -C ₄ H ₉) ₂ ⁵²			10.9	1.92	2.39	38.6	1.401	1.299	112.6	1.373	114.9	1.501	110.7	108.2		
FeFd ₃ (BC ₆ H ₅) ₂ ⁵²			26.4	1.91	2.31	39.2	1.446	1.322	111.0	1.370	113.1	1.496	109.3	109.8		
Fe(CwGm) ₂ (Cl ₂ Gm)(B- <i>n</i> -C ₄ H ₉) ₂	0.36	0.64														
Fe(CwGm) ₃ (B- <i>n</i> -C ₄ H ₉) ₂	0.39	0.63														
Fe((12anS ₄)Gm) ₃ (BC ₆ H ₅) ₂	0.32	0.39														

^a The average of the main structural parameters of chelate cycles. ^b Distance between the coordination polyhedron bases. ^c Bite angle (half of chelate angle). ^d The average of the main structural parameters of capping fragments. ^e Mean deviation of the coordinating nitrogen atoms from C–Fe–C plane. ^f Dihedral angle values for the chelating fragments.

Scheme 2



boron atoms and the iron atom. It should be noted that a reduction of h took place despite the increase in the C–C bond lengths in chelate rings by approximately 0.03–0.04 Å on passing from hexachloride precursors to functionalized clathrochelates (Table 2). The most obvious difference in such bond lengths manifested itself for both types of molecules of nonsymmetrical clathrochelate **11** (Table 2). The octahedral distortion also led to an increase of a torsion angle in the N=C–C=N chelating fragment (and, therefore, to an increase in the displacement Δ of coordinating nitrogen atoms from the C–Fe–C fragment plane), and the symbatic growth in the distortion angle φ (Table 2). In addition, the rotary-translation contraction of a coordination polyhedron on passing from phenylboronic precursor **2** to its derivatives **5**, **6**, and **11** essentially affected the geometry of tetracoordinated boron atoms in the capping groups. The bond angles at these atoms in precursor **2** were indicative of a significant trigonal-pyramidal distortion of an ideal tetrahedron (the coordination polyhedron of boron atoms was elongated along the C_3 axis). At the same time, the trigonal-pyramidal distortion in functionalized clathrochelates **6** and **11** was induced by contraction of the coordination polyhedra of boron atoms along the same axis. The same distortion was also observed in O_3BF fragments of both fluoroboronic precursor **4** and fluoroboronic cobalt clathrochelates.⁵⁴ The bond angles at the boron atom of capping groups in *n*-butylboronic precursor **3** (Table 2) and its derivative **7** and also in thiophenolic complex **5** displayed ideal tetrahedron values.

Among specific features of a crystal arrangement for the clathrochelates under study, one could highlight a parallel mode

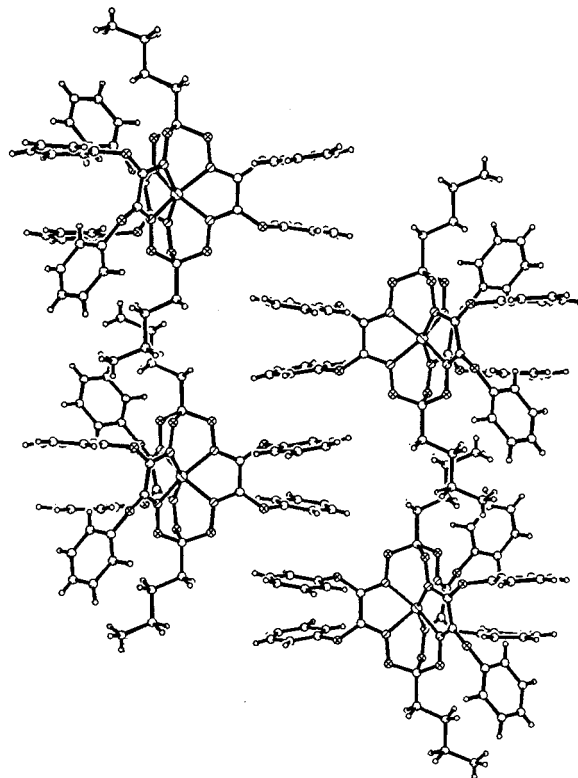


Figure 3. Packing diagram for the molecules of **7**.

of phenoxy substituents in one of the three dioximate fragments of clathrochelate **7** (Figure 3), which may be evidence in favor of π -stacking.

The isomer shift (IS) values, characterizing the s -electron density on the ^{57}Fe nucleus, in the ^{57}Fe Mössbauer spectra of compounds **2–11** obtained are typical for low-spin iron(II) complexes and are practically constant. This indicates a close and high-field force of clathrochelate ligands.

The main specific feature in the UV–vis spectra of low-spin iron(II) tris-dioximates proves to be highly intense $Md \rightarrow L\pi^*$ charge transfer bands (CTB) observed in the visible region. The latter have masked the low-intensity bands of $d-d$ transitions for an Fe^{2+} ion.⁵⁵ As was mentioned earlier,^{47,56,57} for trigonal-antiprismatic complexes in the visible region this proves to be a superimposition of two or more CTBs of close intensity ($\epsilon \sim (3-5) \times 10^3 \text{ mol}^{-1} \text{ L cm}^{-1}$), whereas the trigonal-prismatic compounds are characterized by the presence of one asymmetrical band with a higher intensity ($\epsilon \sim (1.2-3) \times 10^4 \text{ mol}^{-1} \text{ L cm}^{-1}$).

The UV–vis spectra of precursors and their functionalized derivatives with C_3 -symmetrical molecules, like those of all symmetrical macrobicyclic boron-containing iron(II) tris-dioximates with trigonal-prismatic structure, contain an intense CTB in the visible and near-UV region that has two Gaussian components: the main band at 450–550 nm ($\epsilon \sim (1-2) \times 10^4 \text{ mol}^{-1} \text{ L cm}^{-1}$) and an additional one at 390–430 nm with essentially less intensity ($\epsilon \sim (3-7) \times 10^3 \text{ mol}^{-1} \text{ L cm}^{-1}$). In the case of hexachloride precursors **2–4**, phenoxylic and symmetrical oxocrown etheric compounds, the main band has an appreciable (up to 50 nm) UV shift compared with that of

(55) Lever, A. B. P. *Inorganic Electronic Spectroscopy*; Elsevier: Amsterdam, 1984.

(56) Voloshin, Y. Z.; Kostromina, N. A.; Nazarenko, A. Y.; Polshin, E. V. *Inorg. Chim. Acta* **1991**, 185, 83.

(57) Voloshin, Y. Z.; Varzatskii, O. A.; Korobko, S. V.; Maletin, Y. A. *Inorg. Chem. Commun.* **1998**, 1, 328.

(54) Zakrewski, G. A.; Chilardi, C. A.; Lingafelter, E. C. *J. Am. Chem. Soc.* **1971**, 93, 4411.

Table 3. Electrochemical Characteristics and CTB Maxima for Hexachloride Clathrochelate Precursors and Resulting Functionalized Complexes

compound	σ_1^a	σ_{para}^a	methylene dichloride		acetonitrile		λ_{max} , nm
			$E_{1/2}$, mV	Tomeš criterion, mV	$E_{1/2}$, mV	Tomeš criterion, mV	
FeGm ₃ (BC ₆ H ₅) ₂	0 [0.10]	0 [−0.01]	1090	65			438
FeGm ₃ (B- <i>n</i> -C ₄ H ₉) ₂	0 [0.08]	0 [−0.19]	1040	65			439
FeGm ₃ (BF) ₂	0 [0.52]	0 [−0.062]	1250	65			435
Fe(Cl ₂ Gm) ₃ (BC ₆ H ₅) ₂	0.47 [0.10]	0.22 [−0.01]	1360	80			454
Fe(Cl ₂ Gm) ₃ (B- <i>n</i> -C ₄ H ₉) ₂	0.47 [−0.08]	0.227 [−0.19]	1320	90	1320	70	453
Fe(Cl ₂ Gm) ₃ (BF) ₂	0.47 [0.52]	0.227 [0.062]	1415	60	1460	65	451
Fe((C ₆ H ₅ S) ₂ Gm) ₃ (BC ₆ H ₅) ₂	0.27 [0.10]	0.15 [−0.01]	895	80			495
Fe((CH ₃ S) ₂ Gm) ₃ (BC ₆ H ₅) ₂	0.19 [0.10]	0.00 [−0.01]	670	60			498
Fe(<i>n</i> -C ₄ H ₉ NH) ₂ (Gm) ₂ (Cl ₂ Gm)(BC ₆ H ₅) ₂	0.47 (Cl) 0.10 (<i>n</i> -C ₄ H ₉ NH)} 0.22	0.227 (Cl) −0.63 (<i>n</i> -C ₄ H ₉ NH)} −0.34	200	170	90	60	425, 490, 543
Fe((C ₆ H ₅ O) ₂ Gm) ₃ (B- <i>n</i> -C ₄ H ₉) ₂	0.38 [−0.08]	[−0.01] −0.32	795	100			451
Fe(CwGm) ₂ (Cl ₂ Gm)(B- <i>n</i> -C ₄ H ₉) ₂	0.47 (Cl) 0.38 (OC ₆ H ₅)} 0.41	−0.32 (OC ₆ H ₅) 0.227 (Cl)} −0.14	670	65			469, 497
Fe(CwGm) ₃ (B- <i>n</i> -C ₄ H ₉) ₂	0.38 [−0.08]	−0.32 [−0.19]	460	60	420	60	449
Fe((12anS ₄)Gm) ₃ (BC ₆ H ₅) ₂	0.19 [0.10]	0.00 [−0.01]	870	80			504
Fe((CH ₂) ₄ Gm) ₃ (BC ₆ H ₅) ₂ ⁶⁰	−0.05 [0.10]	−0.15 [−0.01]	635				450
Fe((C ₆ H ₅) ₂ Gm) ₃ (B- <i>n</i> -C ₄ H ₉) ₂ ⁶⁰	0.10 [0.08]	−0.01 [−0.19]	760				480
Fe((C ₆ H ₅) ₂ Gm) ₃ (BF) ₂ ⁵⁸	0.10 [0.52]	−0.01 [−0.062]	940	70			479
Fe((CH ₃) ₂ Gm) ₃ (BF) ₂ ⁵⁸	−0.05 [0.52]	−0.17 [−0.062]	785	70			440

^a Taft (σ_1) and Hammett (σ_{para}) constants for substituents in α -dioximate fragments [capping groups]. $\sigma_\Sigma = n/(m+n)\sigma_1 + m/(m+n)\sigma_2$, $\sigma_{n+1} = \sigma_n/2.5$.^{63,64}

sulfur-containing complexes **5**, **6**, and **10** (Table 3). The bands of intraligand $\pi-\pi^*$ transitions for sulfur-containing dioximate fragments in the UV region have a longwave shift (and, therefore, are lower in energy) compared with chlorine- and phenoxy-containing dioximate fragments. For the first approximation, the energy level of the highest occupied iron(II) d orbitals is independent of the nature of the substituent in the dioximate fragment, and the position of CTB is a function of levels of π^* orbitals of this fragment. The decrease in the $\pi-\pi^*$ transition energy in the dioximate fragment led to decreasing CT energy in the iron(II) complex and to a longwave shift of the corresponding band. The main band in the UV-vis spectra of the meridionally asymmetrical *n*-butylaminic complex **11** and partially substituted oxocrown etheric clathrochelate **9** split into two bands of approximately equal intensity. An analogous phenomenon was observed earlier in the spectra of other meridionally asymmetrical iron(II) dioximates.⁵⁸

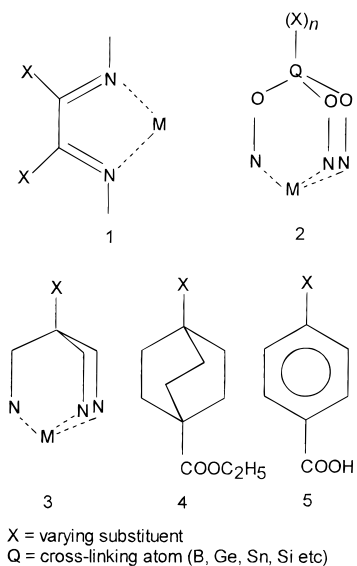
The ¹H and ¹³C NMR spectra of the precursors and the ribbed-functionalized complexes first of all confirmed their composition and the symmetry of the molecule (the presence or absence of the C₃ symmetry axis passing through boron apical atoms and the iron ion). The integral intensities of the ¹H NMR signals of

the substituents in the capping groups and dioximate fragments were in agreement with the supposed composition.

In the case of ¹³C NMR spectra, the signals were assigned with allowance for the previously obtained ¹³C NMR data for such clathrochelate dioximates, the spectra of the starting reactants and model compounds, and the recording of ¹³C NMR spectra with and without decoupling of the spin-spin ¹³C-¹H interaction. It should be noted that despite the electron-accepting character of the chlorine substituent, the chemical shift of the carbon atoms in the azomethine groups of dichloroglyoxime, hexachloride precursors **2-4**, and dichloroglyoximate fragments of partially substituted clathrochelates **9** and **11** is unusually low (≈ 125 ppm). For aromatic, acyclic, and alicyclic dioximes and their complexes, as well as in the case of the synthesized ribbed-functionalized clathrochelates, the $\delta^{13}C(C=N)$ signals were observed in the range 150–160 ppm with the exception of glyoxime and its derivatives, for which $\delta^{13}C(C=N) \approx 140-150$ ppm.^{47,56,58} An extraordinarily low value of $\delta^{13}C(C=N)$ for chloroglyoximates once more confirmed the predominance of a paramagnetic contribution over a diamagnetic one in the chemical shift value on the ¹³C nucleus⁵⁹ and correlated with a decrease in the frequency of the C=N bond stretching vibrations in the IR spectra (see Experimental Section). The $\nu(C=N)$ value in hexachloride complexes is the lowest of all those known so

(58) Voloshin, Y. Z.; Varzatskii, O. A.; Palchik, A. V.; Polshin, E. V.; Maletin, Y. A.; Strizhakova, N. G. *Polyhedron*, **1998**, *17*, 4315.

Scheme 3



far for clathrochelate iron(II) tris-dioximates. The $\nu(\text{C}=\text{N})$ bands of both types of dioximate fragments distinctly appeared in the case of partially substituted meridionally asymmetrical complexes **9** and **11**. Alongside the $\nu(\text{N}-\text{O})$ and $\nu(\text{B}-\text{O})$ bands of the macrobicyclic framework, the IR spectra of functionalized clathrochelates also contained characteristic lines of the incorporated substituents.

Electrochemistry. Cyclic voltammograms of iron(II) clathrochelates are characterized by the existence of anodic waves, which are assigned to the oxidation of iron(II) to iron(III) ions.^{38,60,61} Table 3 lists the half-wave potentials ($E_{1/2}$) attributed to this process, as well as the Tomeš criterion values, that have been determined as a wave slope ($\Delta E = E_{3/4} - E_{1/4}$) and might be used as a characteristic of reversibility and slow of electrochemical reactions (for one-electron reversible process, this value is equal to 56 mV).^{43,44} The data listed indicate that most of the iron(II) clathrochelates obtained have undergone an irreversible oxidation since there are no waves upon backscanning, i.e., oxidation of initial iron(II) clathrochelates was accompanied by further decomposition of the oxidized complex and passivation of the working electrode. This behavior may account for the fact that the stability of iron(III) complexes is much lower than the stability of the initial iron(II) complexes. The size of the cavity in dioximate clathrochelates is optimal for the iron(II) ion, and therefore all attempts to isolate iron(III) clathrochelates by electrolysis at a controlled potential have not been successful. In some cases,⁶¹ upon backscanning it was possible to observe the reduction of oxidation products within the cyclic voltammetry time scale. Among the complexes studied, only in the case of $\text{Fe}((n\text{-C}_4\text{H}_9\text{NH})_2\text{Gm})_2(\text{Cl}_2\text{Gm})\text{-}(\text{BC}_6\text{H}_5)_2$, $\text{Fe}(\text{CwGm})_2(\text{Cl}_2\text{Gm})(\text{B-}n\text{-C}_4\text{H}_9)_2$, and $\text{Fe}((\text{CH}_3\text{S})\text{-}2\text{Gm})_3(\text{BC}_6\text{H}_5)_2$ complexes one can observe the reverse waves that are well reproduced in repeated cycling. It should be noted that the oxidation of the *n*-butylaminic clathrochelate in methylene dichloride occurs as an electrochemically irreversible process ($\Delta E = 170$ mV).

The macrobicyclic complexes of transition metals are known

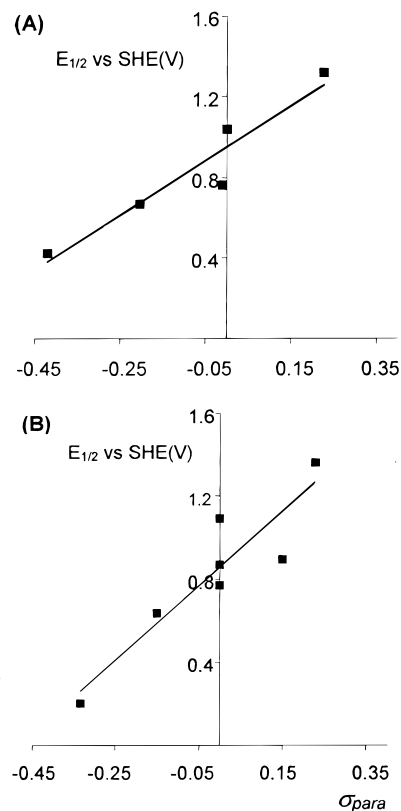


Figure 4. Correlation of $E_{1/2}$ for Fe(III)/Fe(II) couples of the *n*-butylboronic (A) and phenylboronic (B) clathrochelates with Hammett σ_{para} values.

to be quite unique compounds in electron transfer reactions,^{23–28,62} since a coordinately saturated encapsulated metal ion is incapable of coordinating bridged groups, which has not allowed an intraspheric mechanism of the reaction to be realized. The use of substituents of different types in the clathrochelate ligand has permitted considerable changes in the electronic characteristics of the latter and, consequently, wide variations in the redox potential value for the central metal ion. Moreover, quite a variety of apically substituted cobalt sarcophaginates have been proposed for determining the polar substituent σ_{E} constants.⁶²

The tris-dioximate clathrochelates have contained metallobicycles of two types, formed by dioximate fragments with conjugated π bonds (Scheme 3, type 1) and capping groups with a σ -bond system (Scheme 3, types 2 and 3). A correlation between the oxidation half-wave potentials and the inductive constants of substituents has been established for macrobicyclic hexamine complexes (sarcophaginates and sepulchrates), as well as for a series of boron-containing tris-dioximates with different apical substituents.⁹ The Taft inductive constants σ_{I} have been determined⁶³ using saturated bicyclic systems (Scheme 3, type 4). However, it should be noted that the quantitative correlations between the $E_{1/2}$ values and the constants of the substituents have been observed only in the case of reversible processes, i.e., when the magnitude of $E_{1/2}$ coincides with that of the redox potential of the process. As mentioned previously, the oxidation of the clathrochelates obtained is an irreversible process and, therefore, we can deal only with qualitative correlations, typical for these processes.

The $E_{1/2}$ values for the macrobicyclic glyoximates and hexachloride precursors increase in the series $n\text{-C}_4\text{H}_9 < \text{C}_6\text{H}_5$

(59) Breitmaier, E.; Voelter, W. *Carbon-13 NMR Spectroscopy*; VCH: Weinheim, 1987.

(60) Robbins, M. K.; Naser, D. W.; Heiland, J. L.; Grzybowski, J. J. *Inorg. Chem.* **1985**, *24*, 3381.

(61) Voloshin, Y. Z.; Varzatskii, O. A.; Tkachenko, E. Y.; Maletin, Y. A.; Degtyarev, S. P.; Kochubey, D. I. *Inorg. Chim. Acta*, **1997**, *255*, 255.

(62) Lawrence, B. A.; Lay, P. A.; Sargeson, A. M. *Inorg. Chem.* **1990**, *29*, 4808.

(63) Taft, R. W.; Topson, R. D. *Prog. Phys. Org. Chem.* **1987**, *16*, 1.

< F (Table 3). This correlates with the inductive σ_I and Hammett σ_{para} constants. The Hammett constants have been determined⁶⁴ by using substituted benzoic acids (Scheme 3, type 5) and describe both inductive and resonance effects of the substituents. Nevertheless, a correlation coefficient in linear plots of $E_{1/2}$ values versus σ_I is appreciably higher for both groups of complexes.

With substituents in the π -conjugated α -dioximate fragments, the utilization of σ_{para} constants has appeared to be reasonable. Correlations with σ_{para} constants have been established, in particular, for the redox potentials of iron and nickel complexes with tetraene tetraazamacrocyclic ligands.^{65,66}

A number of series of ribbed-functionalized complexes with phenylboronic, *n*-butylboronic, and fluoroboronic capping groups were analyzed. A qualitative correlation between the oxidation half-wave potentials and σ_{para} constants with a coefficient from 0.85 to 0.95 was observed for all three groups of complexes (Figure 4), though there was no correlation between the $E_{1/2}$ values and the inductive σ_I constants. The data for the phenoxy derivative **7** were excluded from the calculations since the oxidation of this complex proceeded irreversibly (the wave slope was 100 mV) and was accompanied by the decomposition of the formed product, and also by passivation of the electrode, which presumably led to an appreciable overvoltage of all processes. No correlation was observed between the $E_{1/2}$ values for the compounds synthesized and the maxima of the CTBs (Table 3).

Summary and Conclusion

Methods of synthesis of reactive hexachloride clathrochelates and ribbed-functionalized polynucleating clathrochelate complexes of different natures have been developed.

The structures of most iron(II) compounds obtained were confirmed by X-ray analysis. The regularities in varying the

main structural parameters of chelate rings and capping groups of clathrochelates during rotary-translational contraction of a trigonal-prismatic coordination polyhedron have been discussed. The complexes synthesized have been characterized by techniques including FAB and PD mass, ⁵⁷Fe Mössbauer, UV-vis, ¹H and ¹³C NMR, and IR spectroscopies and electrochemistry.

The low-spin nature of the clathrochelate obtained and the peculiarities of the electronic d⁶ configuration of the iron(II) ion were determined using ⁵⁷Fe Mössbauer and UV-vis spectroscopic evidence.

The inductive and resonance effects of substituents on the redox potential of the central iron ion were established in both the dioximate fragment and the capping groups. This enabled us to vary this potential over a wide range.

Further studies are now under way to investigate the physicochemical properties of ribbed-functionalized iron(II) clathrochelates and their complexes with metal ions (redox reactions, catalytic activity, extractive ability, and membrane transport) and to synthesize ribbed-functionalized cobalt(III,II) and ruthenium(II) complexes using methods reported here.

Acknowledgment. Support of the Russian Fund of Basic Research (Grants N99-03-32498 and 00-03-32578) is gratefully acknowledged.

Supporting Information Available: Listings of crystal and refinement data, bond distances, angles, and thermal parameters for the complexes **3**, **4**, **6**, **7**, and **11** and figures of the structures **4**, **6**, and **7**. This material is available free of charge via the Internet at <http://pubs.acs.org>.

IC990476N

(65) Goel, R. C.; Henry, P. M.; Polyzou, P. C. *Inorg.Chem.*, **1979**, *18*, 2148.

(66) Streeky, J. A.; Pillsburg, D. G.; Buch, D. H. *Inorg. Chem.* **1980**, *19*, 3148.

(64) Hammett, L. P. *Physical Organic Chemistry: Reaction Rates, Equilibria and Mechanisms*, 2nd ed.; McGraw-Hill: New York, 1970.